Inflationary Quasiparticle Creation and Thermalization Dynamics in Coupled Bose-Einstein Condensates

Anna Posazhennikova,[1,*] Mauricio Trujillo-Martinez,[2] and Johann Kroha[2,3,†]
[1]Department of Physics, Royal Holloway, University of London, Egham, Surrey TW20 0EX, United Kingdom
[2]Physikalisches Institut and Bethe Center for Theoretical Physics, Universität Bonn, Nussallee 12, D-53115 Bonn, Germany
[3]Center for Correlated Matter, Zhejiang University, Hangzhou, Zhejiang 310058, China
(Received 13 April 2016; published 2 June 2016)

A Bose gas in a double-well potential, exhibiting a true Bose-Einstein condensate (BEC) amplitude and initially performing Josephson oscillations, is a prototype of an isolated, nonequilibrium many-body system. We investigate the quasiparticle (QP) creation and thermalization dynamics of this system by solving the time-dependent Keldysh-Bogoliubov equations. We find avalanchelike QP creation due to a parametric resonance between BEC and QP oscillations, followed by slow, exponential relaxation to a thermal state at an elevated temperature, controlled by the initial excitation energy of the oscillating BEC above its ground state. The crossover between the two regimes occurs because of an effective decoupling of the QP and BEC oscillations. This dynamics is analogous to elementary particle creation in models of the early universe. The thermalization in our setup occurs because the BEC acts as a grand canonical reservoir for the quasiparticle system.

DOI: 10.1103/PhysRevLett.116.225304

Common knowledge tells us that many-body systems come to thermodynamic equilibrium by coupling to a heat reservoir. However, how can an *isolated* quantum many-body system eventually come to rest from a given initial nonequilibrium state, and is the final state a thermal one? This is a long-standing problem, which has recently received intense interest [1,2], inspired by the high degree of isolation and control possible in ultracold quantum gases [3,4]. While the unitary time evolution of an isolated quantum system rigorously prohibits the maximization of the total entropy, effective thermalization is generically observed [3,4].

Several mechanisms have been put forward in order to resolve this contradiction, most notably the eigenstate thermalization hypothesis (ETH) [5,6]. It conjectures that for a sufficiently complex quantum system the thermal average of an observable at a given average energy is practically indistinguishable from its expectation value in an eigenstate of the system with that energy. The ETH has been verified numerically for generic, nonintegrable systems and typical observables [7,8], and was found to fail for integrable systems [8,9] with some exceptions [10]. Another mechanism may be termed subsystem thermalization hypothesis (STH). It relies on the fact that, even though total entropy maximization is not possible, subsystems may thermalize by exchanging energy and/or particles with other parts of the system, so that averages of local quantities may be thermal. This mechanism has been successfully invoked [11] even for integrable and nearly integrable systems exhibiting prethermalization dynamics [11–14]. The STH is also at the heart of hydrodynamic behavior, where physical quantities first relax to local averages and then evolve slowly, under the rule of local conservation laws. However, a unified understanding of thermalization has not been reached, and the thermalization mechanism seems to depend strongly on the type of system [8–17].

In the present work we investigate the thermalization dynamics of an interacting Bose gas trapped in a double-well potential which supports a true Bose-Einstein condensate (BEC), initially performing nonequilibrium Josephson oscillations between the two wells [18–21]. This is a prototype of a nonintegrable system with a natural subsystem structure, namely, the BEC and the system of incoherent excitations of Bogoliubov quasiparticles (QPs). The existence of a true BEC phase precludes the system to be one-dimensional. Therefore, and because of the large particle number considered, numerically exact methods, like the time-dependent density-matrix renormalization group (t-DMRG) [12,15], are not applicable here. Moreover, the slow thermalization dynamics found below requires evolving the system to large times, difficult to reach by these methods. Instead, the nonequilibrium Keldysh-Bogoliubov formalism in the grand-canonical ensemble is appropriate here, since the BEC acts as a particle reservoir for the QP system (and vice versa).

We find rich dynamics, governed by three different time scales. After an initial period of undamped Josephson oscillations [22,23], QPs are created in an avalanche manner (QP creation time, τ_c) due to a dynamically generated parametric resonance between the Josephson frequency and the QP excitation energies. This leads to a fast depletion as well as damping of the BEC amplitude [24]. When the final number of QP excitations, allowed by

total energy conservation, is reached, however, the QP system effectively decouples from the BEC oscillations (freeze-out time of the BEC, τ_f), and the total QP number becomes nearly conserved. Under this approximate conservation law the system enters into a quasihydrodynamic regime which is characterized by slow, exponential relaxation of the QP system into a thermalized state (thermalization time, τ_{th}). We prove this behavior by a detailed spectral analysis of the oscillatory behavior in the different time regimes.

Model and formalism.—The Bose gas is described by the Hamiltonian

$$H = \int d\mathbf{r}\hat{\Psi}^\dagger(\mathbf{r},t)\left(-\frac{\nabla^2}{2m} + V_{\text{ext}}(\mathbf{r},t)\right)\hat{\Psi}(\mathbf{r},t) + \frac{g}{2}\int d\mathbf{r}\hat{\Psi}^\dagger(\mathbf{r},t)\hat{\Psi}^\dagger(\mathbf{r},t)\hat{\Psi}(\mathbf{r},t)\hat{\Psi}(\mathbf{r},t), \quad (1)$$

where $\hat{\Psi}(\mathbf{r},t)$ is a bosonic field operator, and $g = 4\pi a_s/m$ is a contact interaction constant, with a_s the s-wave scattering length. V_{ext} is the external double-well trap potential. This system is known to exhibit Josephson oscillations [18–20]. In our approach the condensate is described within a semiclassical two-mode approximation [18], while the QP dynamics are described quantum mechanically [22,23]. We now represent $\hat{\Psi}(\mathbf{r},t)$ in terms of the complete basis $\mathbb{B} = \{\varphi_-, \varphi_+, \varphi_1, \varphi_2, \ldots \varphi_M\}$ of the exact single-particle eigenstates of $V_{\text{ext}}(\mathbf{r})$ after the coupling between the wells is turned on at $t = 0$ by suddenly lowering the barrier between the wells [23]. Hence, for times $t > 0$

$$\hat{\Psi}(\mathbf{r},t) = \phi_1(\mathbf{r})a_1(t) + \phi_2(\mathbf{r})a_2(t) + \sum_{n=1}^{M}\varphi_n(\mathbf{r})\hat{b}_n(t). \quad (2)$$

The first two terms in Eq. (2) constitute the usual two-mode approximation [18], i.e., ϕ_1 and ϕ_2 are symmetric and antisymmetric superpositions of φ_- and φ_+, the ground state and the first excited state of $V_{\text{ext}}(\mathbf{r})$. Hence, the wave function of ϕ_1 (ϕ_2) is localized in the left (right) potential well, and $a_\alpha(t) = \sqrt{N_\alpha(t)}\exp[i\theta_\alpha(t)]$, $\alpha = 1, 2$, are the corresponding BEC amplitudes. This Bogoliubov substitution neglects phase fluctuations in the ground states of each of the potential wells which is justified for sufficiently large BEC particle numbers, $N_\alpha(t) \gg 1$, e.g., for the experiments [19]. For the excited states, φ_n, $n = 1, 2, \ldots, M$, the full quantum dynamics are taken into account by the bosonic creation and destruction operators $\hat{b}_n^\dagger$, $\hat{b}_n$.

For $t > 0$ the Hamiltonian of our system is $H = H_{\text{coh}} + H_J + H_{\text{coll}}$. H_{coh} includes all coherent, local contributions, i.e., all terms which are bilinear in the $\hat{b}_n$ operators and local in the well index $\alpha = 1, 2$,

$$H_{\text{coh}} = \varepsilon_0\sum_{\alpha=1}^{2}a_\alpha^* a_\alpha + \frac{U}{2}\sum_{\alpha=1}^{2}a_\alpha^* a_\alpha^* a_\alpha a_\alpha + \sum_{n=1}^{M}\varepsilon_n\hat{b}_n^\dagger\hat{b}_n + K\sum_{\alpha=1}^{2}\sum_{n,m=1}^{M}\left[a_\alpha^* a_\alpha\hat{b}_n^\dagger\hat{b}_m + \frac{1}{4}(a_\alpha^* a_\alpha^*\hat{b}_n\hat{b}_m + \text{H.c.})\right], \quad (3)$$

where U and K are positive interaction constants, and ε_n are the energies of the M equidistant levels of the double well, separated by the trap frequency, $\varepsilon_n = n\Delta$. For simplicity we neglect here and in the following a possible level dependence of the coupling constants.

H_J encompasses the Josephson terms, which are still coherent but nonlocal in the well index,

$$H_J = -J(a_1^* a_2 + a_2^* a_1) + J'\sum_{n,m=1}^{M}[(a_1^* a_2 + a_2^* a_1)\hat{b}_n^\dagger\hat{b}_m + \frac{1}{2}(a_1^* a_2^*\hat{b}_n\hat{b}_m + \text{H.c.})]. \quad (4)$$

The terms proportional to J' constitute QP-assisted tunneling between the wells.

Finally, the nonlinear collisional terms H_{coll} account for QP interactions,

$$H_{\text{coll}} = \frac{U'}{2}\sum_{n,m=1}\sum_{l,s=1}\hat{b}_m^\dagger\hat{b}_n^\dagger\hat{b}_l\hat{b}_s + R\left[\sum_{\alpha=1}^{2}\sum_{n,m,s=1}a_\alpha^*\hat{b}_n^\dagger\hat{b}_m\hat{b}_s + \sum_{\alpha,\beta,\gamma+1}^{2}\sum_{n=1}a_\alpha^* a_\beta^* a_\gamma\hat{b}_n + \text{H.c.}\right] \quad (5)$$

The time evolution of this system is described in terms of the condensate population imbalance, $z(t) = [N_1(t) - N_2(t)]/[N_1(t) + N_2(t)]$, the phase difference between the BECs, $\theta(t)$ and the QP occupation numbers $n_1(t), n_2(t), \ldots, n_M(t)$. They can be calculated from the classical $\mathbf{C}$ and the quantum $\mathbf{G}$ parts of the two-time Green's functions following standard field-theoretical techniques [25,26],

$$\mathbf{C}_{\alpha\beta}(t_1,t_2) = -i\begin{pmatrix} a_\alpha(t_1)a_\beta^*(t_2) & a_\alpha(t_1)a_\beta(t_2) \\ a_\alpha^*(t_1)a_\beta^*(t_2) & a_\alpha^*(t_1)a_\beta(t_2)\end{pmatrix},$$
$$\mathbf{G}_{nm}(t_1,t_2) = -i\begin{pmatrix} \langle T_C\hat{b}_n(t_1)\hat{b}_m^\dagger(t_2)\rangle & \langle T_C\hat{b}_n(t_1)\hat{b}_m(t_2)\rangle \\ \langle T_C\hat{b}_n^\dagger(t_1)\hat{b}_m^\dagger(t_2)\rangle & \langle T_C\hat{b}_n^\dagger(t_1)\hat{b}_m(t_2)\rangle\end{pmatrix}, \quad (6)$$

where $\hat{T}_C$ denotes time-ordering along the Keldysh contour. The Dyson equations for these functions read

$$\int_C d\bar{t}[\mathbf{G}_0^{-1}(t_1,\bar{t}) - \mathbf{S}^{\mathrm{HF}}(t_1,\bar{t})]\mathbf{C}(\bar{t},t_2) = \int_C d\bar{t}\mathbf{S}(t_1,\bar{t})\mathbf{C}(\bar{t},t_2), \tag{7}$$

$$\int_C d\bar{t}[\mathbf{G}_0^{-1}(t_1,\bar{t}) - \Sigma^{\mathrm{HF}}(t_1,\bar{t})]\mathbf{G}(\bar{t},t_2) = \mathbb{1}\delta(t_1 - t_2) + \int_C d\bar{t}\Sigma(t_1,\bar{t})\mathbf{G}(\bar{t},t_2). \tag{8}$$

In Eqs. (7), (8), the first-order (Hartree-Fock) self-energies $\mathbf{S}^{\mathrm{HF}}$, Σ^{HF} describe time-dependent level renormalizations, while the second-order collisional self-energy contributions $\mathbf{S}$, Σ induce damping of the QP and BEC oscillations. The Dyson equations are expressed in terms of the spectral function $\mathbf{A}_{nm}(t_1,t_2) = i[\mathbf{G}^{>}_{nm}(t_1,t_2) - \mathbf{G}^{<}_{nm}(t_1,t_2)]$ and the statistical function $\mathbf{F}_{nm}(t_1,t_2) = [\mathbf{G}^{>}_{nm}(t_1,t_2) + \mathbf{G}^{<}_{nm}(t_1,t_2)]/2 = \mathbf{G}^{K}_{nm}(t_1,t_2)/2$ and the corresponding self-energies (see Supplemental Material [27]). We solve the resulting integrodifferential equations numerically for total number of particles N_{tot}, level spacing Δ, interactions U, U', K, J', R and initial conditions $z(0)$, $\theta(0)$, with all particles being initially in the BEC, $N_1(0) + N_2(0) = N_{\mathrm{tot}}$. All energies are expressed in units of J: $u = UN_{\mathrm{tot}}/J$, $u' = U'N_{\mathrm{tot}}/J$, $k = KN_{\mathrm{tot}}/J$, $j' = J'N_{\mathrm{tot}}/J$, $r = RN_{\mathrm{tot}}/J$. In the numerical evaluations we limit the number of levels which can be occupied by the QPs to $M = 5$.

BEC and QP dynamics.—Figure 1 shows the dynamics of incoherent excitations for a typical parameter set, given in the figure caption. The time-dependent occupation numbers of all $M = 5$ levels, $n_1, n_2, \ldots, n_M$, and their total,

$$n_{\mathrm{tot}}(t) = \sum_{m=1}^{M} n_m(t) = -\sum_{m=1}^{M}\left[\mathrm{Im}\mathrm{F}^{G}_{mm}(t,t) - \frac{1}{2}\right], \tag{9}$$

are shown. Here F^{G}_{mm} is the regular (upper diagonal) component of the equal-time statistical Green's function $\mathbf{F}_{mm}$ in Bogoliubov space (see Supplemental Material [27]). From Fig. 1 one can readily identify three different dynamical regimes, (I) an early regime of undamped Josephson oscillations without QPs for $t < \tau_c$ [22,23], (II) a fast growth regime of the QP population, and (III) a regime of slow relaxation to a stationary state for long times. In the regimes (II) and (III) the $n_m(t)$ and $n_{\mathrm{tot}}(t)$ oscillate around their respective running mean values, $n_{m,\mathrm{avg}}(t)$ and $n_{\mathrm{avg}}(t)$ (averaged over one oscillation period; smooth lines on top of the oscillating ones). To analyze the functional dependence of this time evolution, we show in Fig. 2 logarithmic plots of the deviation of the total running mean $n_{\mathrm{avg}}(t)$ from its final value $n_{\mathrm{avg}}(\infty)$ (upper panel) and the momentary oscillation amplitude $\Delta n(t) = n_{\mathrm{tot}}(t) - n_{\mathrm{avg}}(t)$ (middle panel) along with the BEC population imbalance $z(t)$ (lower panel). All three quantities show a steep crossover from the fast growth regime (II) to the slow relaxation regime (III) at a freeze-out time scale τ_f, with exponential relaxation for $t > \tau_f$.

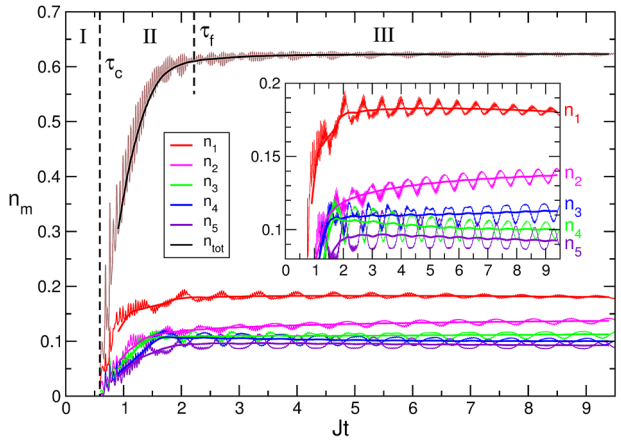

FIG. 1. Dynamics of incoherent excitations for $z(0) = 0.6$, $\theta(0) = 0$, and $\Delta = 9$, $u = u' = 5$, $j' = 40$, $r = 300$, $N_{\mathrm{tot}} = 5 \times 10^5$. n_m is the occupation number of the mth level, n_{tot} is the sum of all $M = 5$ levels. All occupation numbers shown are normalized by the total particle number N_{tot}. The three different dynamical regimes, separated by the characteristic times τ_c and τ_f, are marked, as explained in the text. The inset shows an enlargement of the long-time behavior.

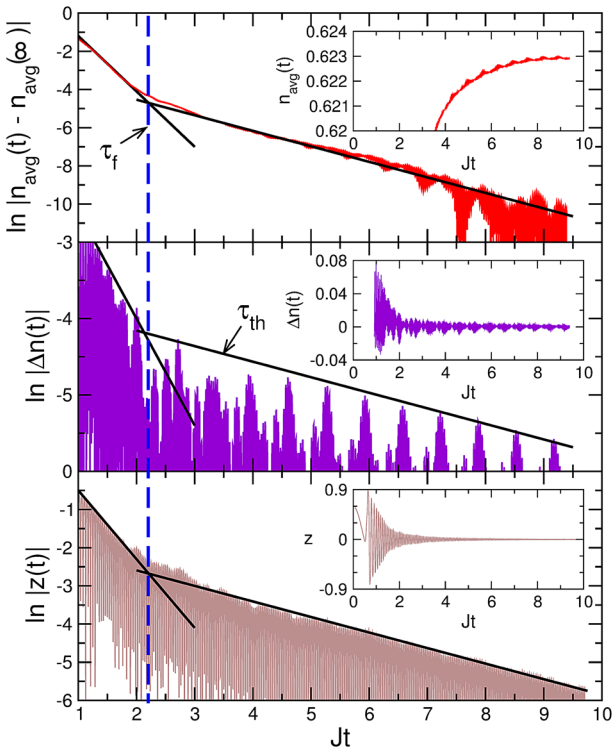

FIG. 2. Logarithmic plots of the relaxation behavior of the QP system (upper two panels) and of the BEC population imbalance (lower panel), see text. The dashed vertical line marks the freeze-out time τ_f where the BEC system and the system of incoherent excitations effectively decouple. The thin, black lines are guides to the eye. The insets show the respective linear plots, for illustration.

What are the mechanisms for fast growth (II) and slow relaxation (III), and how is the steep crossover time τ_f determined? A spectral analysis provides detailed insight into these problems. We introduce the usual Wigner "center-of-motion" (COM) time $t = (t_1 + t_2)/2$ and difference time $\tau = (t_1 - t_2)$ and Fourier transform the two-time Green's functions $A^G(t_1, t_2) = \sum_n A^G_{nn}(t_1, t_2)$ and $F^G(t_1, t_2) = \sum_n F^G_{nn}(t_1, t_2)$ with respect to τ. In Fig. 3 (upper and middle panels) we plot the frequency-dependent absolute values of $A^G(\omega, t) \equiv A(\omega)$ and $F^G(\omega, t) \equiv F(\omega)$ in the long-time regime, $t = 9.01/J > \tau_f$. As expected, the spectra exhibit $M = 5$ approximately Lorentzian peaks corresponding to the five renormalized QP levels. They mark the Rabi oscillation frequencies of the nonequilibrium QP system. Note that, at any instant t of the time evolution, the maximum time interval available for τ is necessarily finite, $-2t < \tau < 2t$ (see Supplemental Material [27]). This limits the frequency resolution of the Fourier transform to $2\pi/4t$ and results in the wiggly modulations of the Lorentzian peaks. For $\tau_c < t < \tau_f$ the spectra look similar, however, with reduced ω resolution (not shown). Figure 3 (lower panel) displays the power spectra of the BEC population imbalance $z(t)$, Fourier transformed with respect to t for $\tau_c < t < \tau_f$ [red curve, regime (II)] and for $t > \tau_f$ [blue curve, enlarged by a factor 10, regime (III)], respectively.

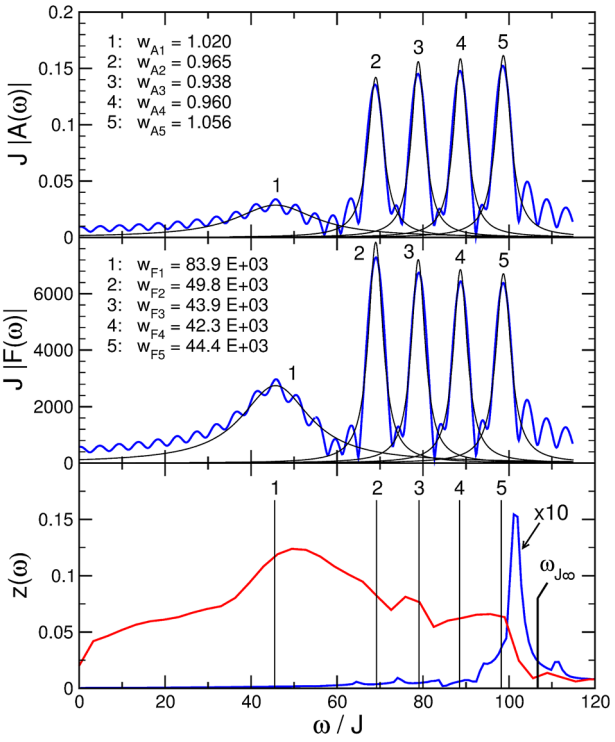

FIG. 3. Absolute values of spectral (upper panel) and statistical (middle panel) functions, Fourier transformed with respect to $\tau = (t_1 - t_2)$ for a fixed value of $t = (t_1 + t_2)/2 = 9.01/J$. The thin, black lines represent Lorentzian fits. The weights w of each of the $M = 5$ Lorentzians are shown in the insets. In the lower panel the power spectrum $z(\omega)$ of the BEC population imbalance is shown for $\tau_c \lesssim t \lesssim \tau_f$ (red line) and for $t > \tau_f$ (blue line). The vertical lines indicate renormalized QP energies. $\omega_{J\infty}$ is the Josephson frequency estimated for the decoupled, quasihydrodynamic regime (see text).

Inflationary QP creation.—In the fast growth regime (II), the BEC oscillation spectrum $z(\omega)$ overlaps strongly with the QP spectrum $|A(\omega)|$ and has even maxima at the renormalized Rabi frequencies. This signals a dynamically generated, parametric resonance, and the strong, resonant QP-BEC coupling leads to the inflationary QP generation observed in Fig. 1.

Approach to stationary state.—In the long-time regime (III), the behavior is strikingly different: the spectrum of the BEC oscillations exhibits a single, sharp peak of substantially reduced weight which has almost no overlap with the QP spectrum. In fact, the BEC oscillation frequency is close to the Josephson frequency $\omega_{J\infty}$ of a semiclassical, interacting BEC, i.e. *without* locking to the QP oscillations. ω_{J_∞} may be estimated as [18], $\omega_{J\infty} \approx 2J_{\rm eff}\sqrt{1 + uJ/(2J_{\rm eff})}$, where $J_{\rm eff} = J + n_{\rm tot}(t \to \infty)J'$ is the QP-enhanced Josephson coupling. It is marked in Fig. 3 by the thick, vertical line. Therefore, in the long-time regime the BEC system performs nearly free, weakly damped (due to the sharpness of the spectral peak) oscillations at nearly its own eigenfrequency $\omega_{J\infty}$. That is, for $t > \tau_f$ the BEC and the QP subsystems are effectively decoupled.

The mechanism for this freeze-out of BEC oscillations may now be interpreted as a combination of total energy conservation and a maximum entropy principle in the QP subsystem. The latter implies that $n_{\rm tot}(t)$ can essentially not decrease (up to small oscillations induced by the BEC driving). The energy $E_{\rm QP}(t)$ of the QP subsystem increases continuously with the occupation numbers $n_m(t)$, but is limited by the maximum energy that can be provided by the BEC system, i.e., by the difference between the BEC energies in the initial and in the final state, $\Delta E_{\rm BEC} = E_{\rm BEC}(t = 0) - E_{\rm BEC}(t \to \infty)$ (see Supplemental Material [27]). We find numerically that $E_{\rm QP}(t)$ indeed approaches this maximum value at $t \approx \tau_f$. Hence, for $t > \tau_f$, $n_{\rm tot}(t)$ and $E_{\rm QP}(t)$ become approximately conserved in the grand canonical sense, i.e., particle and energy exchange with the BEC are allowed, but the time averages are approximately constant; cf. Fig. 1. As a consequence, the resonant dynamics of the BEC and the QP systems must decouple, as seen from Fig. 3. Under these dynamically generated, approximate conservation laws the system enters into a quasihydrodynamic regime, characterized by slow, exponential relaxation, where only a redistribution of QPs between the individual QP levels occurs.

Thermalization.—To test if the long-time stationary state is a thermal one, we calculate the QP distribution $b(\varepsilon_n, t)$ for different COM times t. It is defined via the Green's functions [25] by $F(\omega, t) = (-i/2)[2b(\omega, t) + 1]A(\omega, t)$ and, hence, is obtained for each level from the Lorentzian weights $w_{A,n}$, $w_{F,n}$ of these levels (cf. Fig. 3) as

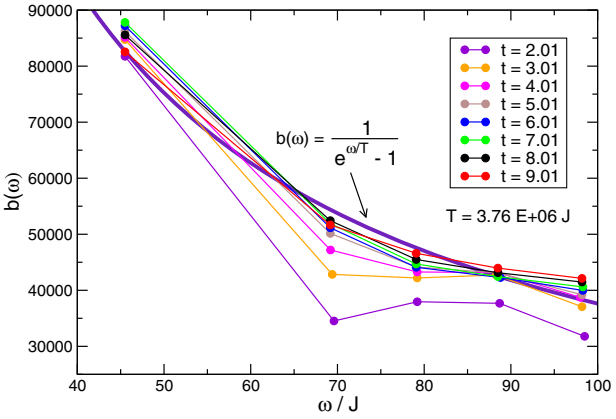

FIG. 4. Distribution function $b(\tilde{\varepsilon}_n, t)$ for different COM times t. The thick purple line is a single-parameter fit of a thermal distribution to the calculated $b(\tilde{\varepsilon}_n, t)$ for the largest time $t = 9.01$, with temperature T as fit parameter. The fitted value is $T = 3.76 \times 10^6\ J$.

$$b(\tilde{\varepsilon}_n, t) = \frac{w_{F,n}}{w_{A,n}} - \frac{1}{2}. \tag{10}$$

$\tilde{\varepsilon}_n$, $n = 1, \ldots, M$, are the level energies, renormalized by interactions. As shown in Fig. 4, $b(\tilde{\varepsilon}_n, t)$ continuously approaches a thermal distribution. For large t this happens only by a redistribution of weights among the levels, without total particle number increase. For even longer times the agreement with a thermal distribution will be even better, since, e.g., the occupations $n_2(t)$, $n_3(t)$ are still growing, while $n_5(t)$ is still decreasing even for the longest time shown, as seen in Fig. 1. As expected, the final-state temperature T is high, since it is controlled by the initial BEC excitation energy, $\Delta E_{\mathrm{BEC}} \sim z(0)^2 N_{\mathrm{tot}} J$, which is a macroscopically large quantity.

To conclude, the system of coupled, oscillating BECs and incoherent excitations thermalizes, because the condensates serve as a heat reservoir for the quasiparticle subsystem. The condensate oscillations, in turn, get damped by quasiparticle collisions. By studying the system dynamics we found a steep coupling-decoupling crossover of the condensate and the quasiparticle subsystems at the freeze-out time scale τ_f. Prior to τ_f, the condensate and the quasiparticles are strongly coupled as a result of a dynamically generated parametric resonance. For times $t > \tau_f$, BEC and incoherent excitations exhibit off-resonant behavior and are effectively decoupled. This freeze-out occurs as a consequence of total energy conservation and entropy maximization in the quasiparticle subsystem. In the off-resonant regime, the quasiparticle system relaxes slowly to a thermalized state with thermalization time $\tau_{th} \gg \tau_f$. The BEC freeze-out and subsequent time evolution under a conservation law are reminiscent of prethermalization found in low-dimensional, nearly integrable systems. However, here the conservation law is generated dynamically in a nonintegrable system. The quasiparticle dynamics bears similarities to models for the resonant creation and subsequent freeze-out of elementary particles during the evolution of the early universe [28].

*anna.posazhennikova@rhul.ac.uk
†kroha@th.physik.uni-bonn.de

[1] A. Polkovnikov, K. Sengupta, A. Silva, and M. Vengalattore, Rev. Mod. Phys. **83**, 863 (2011).
[2] J. Eisert, M. Friesdorf, and C. Gogolin, Nat. Phys. **11**, 124 (2015).
[3] S. Trotzky, Y.-A. Chen, A. Flesch, I. P. McCulloch, U. Schollwöck, J. Eisert, and I. Bloch, Nat. Phys. **8**, 325 (2012).
[4] M. Gring, M. Kuhnert, T. Langen, T. Kitagawa, B. Rauer, M. Schreitl, I. Mazets, D. A. Smith, E. Demler, and J. Schmiedmayer, Science **337**, 1318 (2012).
[5] J. M. Deutsch, Phys. Rev. A **43**, 2046 (1991).
[6] M. Srednicki, Phys. Rev. E **50**, 888 (1994).
[7] M. Rigol, V. Danjko, and M. Olshanii, Nature (London) **452**, 854 (2008).
[8] M. Rigol and M. Srednicki, Phys. Rev. Lett. **108**, 110601 (2012).
[9] M. Rigol, Phys. Rev. Lett. **103**, 100403 (2009).
[10] V. Alba, Phys. Rev. B **91**, 155123 (2015).
[11] F. H. L. Essler, G. Mussardo, and M. Panfil, Phys. Rev. A **91**, 051602 (2015).
[12] C. Kollath, A. M. Läuchli, and E. Altman, Phys. Rev. Lett. **98**, 180601 (2007).
[13] M. Moeckel and S. Kehrein, Phys. Rev. Lett. **100**, 175702 (2008).
[14] M. Kollar, F. A. Wolf, and M. Eckstein, Phys. Rev. B **84**, 054304 (2011).
[15] Th. Barthel and U. Schollwöck, Phys. Rev. Lett. **100**, 100601 (2008).
[16] V. Yukalov, Laser Phys. Lett. **8**, 485 (2011).
[17] A. Riera, C. Gogolin, and J. Eisert, Phys. Rev. Lett. **108**, 080402 (2012).
[18] A. Smerzi, S. Fantoni, S. Giovanazzi, and S. R. Shenoy, Phys. Rev. Lett. **79**, 4950 (1997).
[19] M. Albiez, R. Gati, J. Fölling, S. Hunsmann, M. Cristiani, and M. K. Oberthaler, Phys. Rev. Lett. **95**, 010402 (2005).
[20] S. Levy, E. Lahoud, I. Shomroni, and J. Steinheuer, Nature (London) **449**, 579 (2007).
[21] L. J. LeBlanc, A. B. Bardon, J. McKeever, M. H. T. Extavour, D. Jervis, J. H. Thywissen, F. Piazza, and A. Smerzi, Phys. Rev. Lett. **106**, 025302 (2011).
[22] M. Trujillo-Martinez, A. Posazhennikova, and J. Kroha, Phys. Rev. Lett. **103**, 105302 (2009).
[23] M. Trujillo-Martinez, A. Posazhennikova, and J. Kroha, New J. Phys. **17**, 013006 (2015).
[24] V. I. Yukalov and E. P. Yukalova, Phys. Rev. A **78**, 063610 (2008).
[25] J. Rammer, *Quantum Field Theory of Non-equilibrium States* (Cambridge University Press, Cambridge, England, 2007).
[26] A. Griffin, T. Nikuni, and E. Zaremba, *Bose-Condensed Gases at Finite Temperatures* (Cambridge University Press, Cambridge, England, 2009).
[27] See Supplemental Material at http://link.aps.org/supplemental/10.1103/PhysRevLett.116.225304 for details of the formalism and numerical evaluation.
[28] L. Kofman, A. Linde, and A. A. Starobinsky, Phys. Rev. Lett. **73**, 3195 (1994).